フォスファチジルイノシトール3リン酸（以下PI3K）も候補にあげられる。PI3Kはその上流の受容体型チロシンキナーゼやRASにより活性化されるが，自身の触媒または調節ドメインに対応する遺伝子変異によっても活性化され，PI3K/Akt経路の活性化を介して細胞死を抑制する機能を担う。

PI3Kの触媒サブユニットのp110αをコードする*PIK3CA*遺伝子には，乳癌，尿路系癌，子宮癌，大腸癌，頭頸部癌などで変異がみつかり注目されている[18,19]。大腸癌では*PIK3CA*遺伝子の変異は15%程度の頻度で，その変異は1塩基置換を生じるものが多く，exon 9（E542K，E545Kなど）および20（H1047Rなど）を解析することで80%以上を網羅できるとされている[13]。ただ，*PIK3CA*遺伝子の変異については，抗EGFR抗体薬の治療成績に関連性があるという報告[20]と関連性がない[21]という相反する報告があり，治療成績との関連は今のところ不確定である。また，exon 20の変異のみが治療効果予測因子になり得るという報告もある[22]。

また，PI3Kの調節サブユニットのp85αをコードする*PIK3R1*遺伝子に関しても大腸癌で約8%の頻度で変異があったと報告されている[23]。*PIK3CA*遺伝子と同様，治療成績との関連は今のところ不確定である。

V．PTEN

*PTEN*はPI3K/Akt経路を阻害するがん抑制遺伝子であり，PI3Kを脱リン酸化する。*PTEN*遺伝子の変異は様々な癌で報告されている[24]。また，PTENの発現消失は20～30%前後の大腸癌に認められている。臨床研究においては，原発巣ではPTENの発現の有無でcetuximab投与の治療成績は変わらないものの，転移巣ではPTEN発現患者で治療成績が良好であったとの報告がある[25,26]。

また免疫組織化学染色法でのPTEN非発現患者は，後ろ向き研究の結果ではあるが，*KRAS*・*BRAF*遺伝子ともに野生型の患者におけるcetuximab治療で，治療効果予測因子にはならないものの，不良な予後予測因子であったと報告されている[27]。

Ⅵ．Amphiregulin，epiregulin

amphiregulin（以下AREG）やepiregulin（以下EREG）はEGFRのリガンドであり，EGF，TGFαよりも結合能が弱いことが知られている。ただし，進行・再発大腸癌における予後予測因子あるいは抗EGFR抗体薬の治療効果予測因子である可能性が報告されており，がん化の過程で中心的な役割を果たしていると考えられる。

*KRAS*遺伝子変異のように治療効果が期待できない患者を選別する役割を果たすことは難しいが，*KRAS*野生型においてAREGやEREGが高発現している場合，cetuximab＋irinotecan併用療法を行うことで良好な治療成績が得られると報告された[28]。*KRAS*変異型では，AREGやEREGの発現と治療成績に相関は認めなかった。

Ⅶ．抗EGFR抗体とADCC活性

ADCCとは，標的細胞に結合した抗体がナチュラルキラー細胞やT細胞，好中球，マクロファージなどのエフェクター細胞上のFc受容体と結合することで，抗体依存的に誘導される標的細胞介在性傷害活性である。抗CD20抗体（rituximab），抗HER2抗体（trastuzumab）をはじめとするIgG_1サブクラスの抗体薬治療に特異的な利点として注目されており，Fcγ受容体の遺伝子多型により治療成績に差が生じることが報告されている[29,30]。IgG_1抗体であるcetuximabにおいても，EGFR依存性シグナル伝達経路の阻害の他にADCCの誘導が寄与していることが知られており[31,32]，*FcγRⅡa*と*FcγRⅢa*の遺伝子多型（FcγⅡa-H/R[131]，FcγRⅢa-V/F[158]）に影響を受けるとされている。そのため，Fcγ受容体の遺伝子多型はIgG_1サブクラスであるcetuximabの治療効果予測のための分子マーカーとして期待されている。

FcγRⅡa，*Ⅲa*遺伝子については，欧米からの報告[33]によりcetuximabに対してより高い治療成績が期待されている遺伝子型は131H，158Vであり，これはrituximab，trastuzumabで示された傾向と一致している。HapMapプロジェクトによると日本人におけるH/Hの遺伝子型は約70%を占めるとされており，この頻度は欧米人に比し高頻度である。反対にV/Vの遺伝子型は約2%であり，この頻度は欧米人に比しやや低頻度である。*FcγRⅡa*，*Ⅲa*遺伝子を総合で考えると，cetuximabの治療成績が期待される遺伝子多型をもつ頻度は，日本人において欧米人よりもやや多く，ADCC活性が治療成績に影響すると仮定するならば，欧米人に比し日本人は良好な治療成績が期待できると考えられる。

Ⅷ．抗EGFR抗体薬投与における皮膚症状

抗EGFR抗体薬において皮膚障害は最も頻度の高い毒性であり，grade 2以上の皮膚障害はその治療成績に関連すると報告されている[34]。ただし，抗EGFR抗体薬による治療経過中の最高gradeと治療成績を比較している報告が大部分であり，治療が長期間に及び総投与量が多くなる患者が，より高度のgradeに分類されやすくなっている可能性がある。そのため，皮膚障害が治療効

果予測因子になり得ると厳密には結論付けられないと考えられる。皮膚障害と治療成績の関連性を新たに示すためには，治療開始後早期に期間を限定した皮膚障害のgradeの解析が今後必要になると考えられる。

おわりに

現在，患者の個別化医療分野において，薬剤の効果を予測するバイオマーカーを開発することは最も重要な課題の一つである。抗EGFR抗体薬の治療成績は，*KRAS*遺伝子変異の有無により大きく異なることが明らかになり，大腸癌の薬物療法に初めて個別化医療が導入された。今後，*KRAS*遺伝子同様に*BRAF*遺伝子や*PIK3CA*遺伝子などについてもバイオマーカーとなり得るか検討することは，大腸癌の個別化治療をさらに前進させるものと期待される。バイオマーカーを用いたがん分子標的治療薬による治療を行うためには様々な臨床試験による検証が必要であるが，治療効果を最大限に引きだし副作用を軽減することで，患者のケアに劇的な改善をもたらし，さらに医療費削減にも貢献できるものと考えられる。

文　献

1) Kopetz S, Chang GJ, Overman MJ, *et al*: Improved survival in metastatic colorectal cancer is associated with adoption of hepatic resection and improved chemotherapy. *J Clin Oncol* **27**: 3677-3683, 2009.
2) Scaltriti M and Baselga J: The epidermal growth factor receptor pathway: a model for targeted therapy. *Clin Cancer Res* **12**: 5268-5272, 2006.
3) Yarden Y and Sliwkowski MX: Untangling the ErbB signalling network. *Nat Rev Mol Cell Biol* **2**: 127-137, 2001.
4) McCubrey JA, Steelman LS, Abrams SL, *et al*: Roles of the RAF/MEK/ERK and PI3K/PTEN/AKT pathways in malignant transformation and drug resistance. *Adv Enzyme Regul* **46**: 249-279, 2006.
5) Li S, Schmitz KR, Jeffrey PD, *et al*: Structural basis for inhibition of the epidermal growth factor receptor by cetuximab. *Cancer Cell* **7**: 301-311, 2005.
6) Hecht JR, Mitchell E, Neubauer MA, *et al*: Lack of correlation between epidermal growth factor receptor status and response to panitumumab monotherapy in metastatic colorectal cancer. *Clin Cancer Res* **16**: 2205-2213, 2010.
7) Downward J: Targeting RAS signaling pathways in cancer therapy. *Nat Rev Cancer* **3**(1): 11-22, 2003.
8) Brink M, de Goeij AF, Weijenberg MP, *et al*: K-ras oncogene mutations in sporadic colorectal cancer in The Netherlands Cohort Study. *Carcinogenesis* **24**: 703-710, 2003.
9) Egan SE and Weinberg RA: The pathway to signal achievement. *Nature* **365**: 781-783, 1993.
10) Cutsem EV, Kohne CH, Hitre E, *et al*: Cetuximab and chemotherapy as initialtreatment for metastatic colorectal cancer. *N Engl J Med* **360**: 1408-1417, 2009.
11) Bokemeyer C, Bondarenko I, Makhson A, *et al*: Fluorouracil leucovorin, and oxaliplatin with and without cetuximab in the first-line treatment of metastatic colorectal cancer. *J Clin Oncol* **27**: 663-671, 2009.
12) Michaloglou C, Vredeveld LCW, Mooi WJ, *et al*: $BRAF^{E600}$ in benign and malignant human tumours. *Oncogene* **27**: 877-895, 2008.
13) Barault L, Veyrie N, Jooste V, *et al*: Mutations in RAS-MAPK, PI3K signaling network correlate with poor survival in a population-based series of colon cancers. *Int J Cancer* **122**: 2255-2259, 2008.
14) Davies H, Bignell GR, Cox C, *et al*: Mutations of the BRAF gene in human cancer. *Nature* **417**: 949-954, 2002.
15) Di Nicolantonio F, Martini M, Molinari F, *et al*: Wild-type *BRAF* is required for response to panitumumab or cetuximab in metastatic colorectal cancer. *J Clin Oncol* **26**: 5705-5712, 2008.
16) Loupakis F, Ruzzo A, Cremolini C, *et al*: KRAS codon 61, 146 and BRAF mutations predict resistance to cetuximab plus irinotecan in KRAS codon 12 and 13 wild-type metastatic colorectal cancer. *Br J Cancer* **101**: 715-721, 2009.
17) Tol J, Nagtegaal ID, Punt CJ, *et al*: BRAF mutation in metastatic colorectal cancer. *N Engl J Med* **361**: 98-99, 2009.
18) Roberts PJ and Der CJ: Targeting the Raf-MEK-ERK mitogen-activated proitein kinase cascade for the treatment of cancer. *Oncogene* **26**: 3291-3310, 2007.
19) Bader AG, Kang S, Zhao L, *et al*: Oncogenic PI3K deregulates transcription and translation. *Nat Rev Cancer* **5**: 921-929, 2005.
20) Sartore-Bianchi A, Martini M, Molinari F, *et al*: PIK3CA mutations in colorectal cancer are associated with clinical resistance to EGFR-targeted monoclonal antibodies. *Cancer Res* **69**(5): 1851-1857, 2009.
21) Prenen H, De Schutter J, Jacobs B, *et al*: PIK3CA mutations are not a major determinant of resistance to the epidermal growth factor receptor inhibitor cetuximab in metastatic colorectal cancer. *Clin Cancer Res* **15**: 3184-3188, 2009.
22) De Roock W, Claes B, Bernasconi D, *et al*: Effects of KRAS, BRAF, NRAS, and PIK3CA mutations on the efficacy of cetuximab plus chemotherapy in chemotherapy-refractory metastatic colorectal cancer: a retrospective consortium analysis. *Lancet Oncol* **11**: 753-762, 2010.
23) Jaiswal BS, Janakiraman V, Kljavin NM, *et al*: Somatic mutation in p85α promote tumorigenesis through class IA PI3K activation. *Cancer Cell* **16**: 463-474, 2009.
24) Keniry M and Parsons R: The role of PTEN signaling perturbations in cancer and in targeted therapy. *Oncogene* **27**: 5477-5485, 2008.
25) Loupakis F, Pollina L, Stasi I, *et al*: PTEN expression and KRAS mutations on primary tumors and metastases in the prediction of benefit from cetuximab plus irinotecan for patients with metastatic colorectal cancer. *J Clin Oncol* **27**: 2622-2629, 2009.
26) Negri FV, Bozzetti C, Lagrasta CA, *et al*: PTEN status in advanced colorectal cancer treated with cetuximab. *Br J Cancer* **102**: 162-164, 2010.
27) Laurent-Puig P, Cayre A, Manceau G, *et al*: Analysis of PTEN, BRAF, and EGFR status in determining benefit from cetuximab therapy in wild-type KRAS metastatic colon cancer. *J Clin Oncol* **27**(35): 5924-5930, 2009.
28) Jacobs B, De Roock W, Piessevaux H, *et al*: Amphiregulin and epiregulin mRNA expression in primary tumors predicts outcome in metastatic colorectal cancer treated with cetuximab. *J Clin Oncol* **27**(30): 5068-5074, 2009.
29) Cartron G, Dacheux L, Salles G, *et al*: Therapeutic activity of humanized anti-CD20 monoclonal antibody and polymorphism in IgG Fc receptor FcγRⅢa gene. *Blood* **99**: 754-758, 2002.
30) Weng WK and Levy R: Two immunoglobulin G fragment C receptor polymorphisms independently predict

response to rituximab in patients with follicular lymphoma. *J Clin Oncol* **21**: 3940-3947, 2003.
31) Kawaguchi Y, Kono K, Mimura K, *et al*: Cetuximab induce antibody-dependent cellular cytotoxicity against EGFR-expressing esophageal squamous cell carcinoma. *Int J Cancer* **120**: 781-787, 2007.
32) Kimura H, Sakai K, Arao T, *et al*: Antibody-dependent cellular cytotoxicity of cetuximab against tumor cells with wild-type or mutant epidermal growth factor receptor. *Cancer Sci* **98**: 1275-1280, 2007.
33) Bibeau F, Lopez-Crapez E, Di Fiore F, *et al*: Impact of FcγR II a-FcγR III a polymorphisms and *KRAS* mutations on the clinical outcome of patients with metastatic colorectal cancer treated with cetuximab plus irinotecan. *J Clin Oncol* **27**: 1122-1129, 2009.
34) Jonker DJ, O'Callaghan CJ, Karapetis CS, *et al*: Cetuximab for the treatment of colorectal cancer. *N Engl J Med* **357**(20): 2040-2048, 2007.

Cancer Science
The official journal of the Japanese Cancer Association JCA

Contribution of autophagic cell death to p53-dependent cell death in human glioblastoma cell line SF126

Yasuhiro Sakamoto, Shunsuke Kato, Masahiro Takahashi, Yoshinari Okada, Katsuhiro Yasuda, Gou Watanabe, Hiroo Imai, Atsuko Sato and Chikashi Ishioka[1]

Department of Clinical Oncology, Research Institute of Development, Aging and Cancer, Tohoku University, Sendai, Japan

(Received August 25, 2010/Revised December 20, 2010/Accepted December 23, 2010/Accepted manuscript online January 8, 2011/Article first published online February 11, 2011)

Apoptosis and autophagic cell death are programmed cell deaths that are involved in cell survival, growth, development and carcinogenesis. p53, the most extensively studied tumor suppressor, regulates apoptosis and autophagy by transactivating its downstream genes. It also stimulates the mitochondrial apoptotic pathway and inhibits autophagy in a transactivation-independent manner. However, the contribution of apoptosis and autophagic cell death to p53-dependent cell death is unclear. Using wild-type (WT) and mutant (MT) p53 inducible cell lines in *TP53*-null SF126 glioblastoma cells, we examined the apoptosis and autophagic cell death induced by p53. WT p53 expression in SF126 cells induced apoptosis and autophagy, and reduced the cell number. An autophagy inhibitor reduced autophagy, increased the S-phase fraction, and attenuated the inhibition of cell proliferation induced by WT p53. Pan-caspase inhibitor reduced apoptosis but showed weaker inhibition of cell proliferation than the autophagy inhibitor. We concluded that p53-dependent cell death in SF126 cells comprises caspase-dependent and caspase-independent apoptosis and autophagic cell death, and the induction of autophagy as well as apoptosis could be a new strategy to treat some type of WT p53-retaining tumors. (*Cancer Sci* 2011; 102: 799–807)

Both apoptosis and autophagic cell death are included in programmed cell death. They are involved in not only cell homeostasis processes such as cell survival, growth and development, but also cancer progression and proliferation. Classical chemotherapeutic drugs target DNA to eliminate cancer cells by inducing DNA damage and subsequent apoptosis. Current molecular target drugs also activate the apoptotic pathway, but recent study shows some of these classical drugs and molecular target drugs are also involved in the autophagic pathway.[1,2]

Apoptosis is a well-known programmed cell death. Morphological features of apoptosis include membrane changes, chromatin condensation, nuclear fragmentation and apoptotic body formation.[3] On the other hand, autophagy is a bulk degradation mechanism that plays an essential role in the removal and recycling of cytoplasmic proteins and organelles as well as the maintenance of cellular nutrient homeostasis during nutrient deprivation. Morphological features of autophagy are the formation of a closed double membrane vacuole called an autophagosome, which matures by fusion with a lysosome to create an autolysosome. Although autophagy is necessary for cell survival, recent studies have demonstrated that it induces cell death under specific circumstances such as cancer.[4–6] Cell death with the morphological feature of autophagy is defined as autophagic cell death. In cell death due to autophagy, the fate of the cell should be altered and result in long-term cellular survival when an autophagy inhibitor (such as 3-methyladenine) or siRNA of an autophagy-related gene (such as *Atg5*) inhibits autophagy.[7] Autophagy removes harmful proteins and organelles that induce DNA damage in a cell; therefore, it works against carcinogenesis. Indeed, *beclin-1*, a phylogenetically conserved autophagy-related gene, is often inactivated monoallelically in human cancers.[8] Furthermore, *beclin-1*$^{+/-}$ mutant mice suffer from a high incidence of spontaneous tumors.[9] These indicate that *beclin-1* is a haploinsufficient tumor suppressor gene.

Tumor suppressor p53 regulates both apoptosis and autophagy.[10] p53 is activated by a variety of cellular genotoxic stressors[11] and subsequently, p53 transactivates apoptosis- and autophagy-inducing genes (apoptosis: *BAX*,[12] *p53AIP1*[13] and *PUMA*;[14] and autophagy: *DRAM*,[15] *Sestrin 1* and *Sestrin 2* [*SESN 2*][16,17]). Moreover, p53 also regulates apoptosis and autophagy in a transactivation-independent manner. Cytoplasmic p53 induces mitochondrial outer membrane permeabilization, followed by the release of cytochrome c and subsequent apoptosis,[18,19] and attenuated the induction of autophagy.[20,21]

Although p53 regulates both apoptosis and autophagy by diverse mechanisms, it remains unclear how much they contribute to actual p53-dependent cell death and inhibition of cell proliferation. Furthermore, whether the apoptosis and autophagy induced by p53 are mutually independent is unclear. To answer these questions, we constructed a wild-type (WT) p53-inducible cell line in SF126 glioblastoma cells and analyzed the contribution of apoptosis and autophagy to WT p53-dependent cell death using apoptosis and autophagy inhibitors. We also established S121F and R306G mutant (MT) p53-inducible cell lines and analyzed the contribution of apoptosis and autophagy the same as WT p53. These two mutants have not been reported in human tumor. But the cell biological behaviors of these mutants are interesting. S121F has a stronger apoptosis-inducing ability than WT p53.[22] R306G localizes in the cytoplasm due to lack of association to importin alpha, and the truncated form of importin alpha is identified in breast cancer,[23] and might have a strong autophagy-inhibiting ability because of its cytoplasmic localization.[20,21] We considered that comparing the phenotypes of MT p53 to WT p53 might be useful for assessing if apoptosis and autophagy are functionally independent from each other.

Materials and Methods

Cell lines and cell culture. The stable SF126 cell line expressing doxycycline (Dox)-inducible WT p53 (SF126-tet-p53: WT clone) was previously constructed.[24] SF126-tet-TON (Mock clone), SF126-tet-S121F (S121F clone) and SF126-tet-R306G (R306G clone) were constructed according to the protocol described in a previous report[24] using the three plasmids, pcDNA5/TON, pcDNA5/TON-p53S121F and pcDNA5/

[1]To whom correspondence should be addressed.
E-mail: chikashi@idac.tohoku.ac.jp

doi: 10.1111/j.1349-7006.2011.01857.x

TON-p53R306G, respectively.[25] Wild-type or MT p53 was induced with 10 ng/mL Dox (Sigma-Aldrich, St. Louis, MO, USA). For inhibition of autophagy and apoptosis, cells were cultured with 6 mM 3-methyladenine (3MA; Sigma-Aldrich) and 10 μM benzyloxycarbonyl-valyl-alanyl-aspartic acid (O-methyl)-fluoro-methylketone (VAD; R&D systems, Minneapolis, MN, USA), respectively.

Subcellular fractionation. Before trypsinization, cells were washed once in cold phosphate-buffered saline (PBS), lysed and separated into subcellular fractions using the CelLytic NuCLEAR Extraction kit (Sigma-Aldrich) following the manufacturer's recommendations.

Western blotting analysis. Cells were harvested and resuspended in lysis buffer containing 50 mM Tris–HCl (pH 8.0), 150 mM NaCl, 5 mM EDTA and 1% protease inhibitor cocktail (Sigma-Aldrich). The lysate was analyzed by western blotting as described previously[26] using anti-p53 (sc-6243; Santa Cruz Biotechnology, Santa Cruz, CA, USA), anti-actin (A2066; Sigma-Aldrich), anti-LC3 (PM036; Medical & Biological Laboratories, Nagoya, Japan), anti-BAX (M010-3; Medical & Biological Laboratories), anti-DRAM (ab72171; Abcam, Cambridge, MA, USA), anti-14-3-3σ (ab14123; Abcam), anti-SESN2 (ab57810; Abcam), anti-MDM2 (sc-965; Santa Cruz Biotechnology) and anti-p21 (sc-397; Santa Cruz Biotechnology) antibodies.

Immunofluorescence analysis. The strategy for p53 immunofluorescence was described in a previous report.[24] For LC3 immunofluorescence, cells were harvested at 18 h after treatment and fixed with 4% paraformaldehyde and incubated for 10 min at room temperature. After washing with PBS, they were then permeabilized with 50 μg/mL digitonin (Sigma-Aldrich) for 15 min at room temperature. After washing with PBS, these cells were incubated with anti-LC3 (PM036; Medical & Biological Laboratories) diluted 1:250 for 1 h. After washing with PBS, they were incubated with Anti-Rabbit IgG(H + L)FITC (Beckman Coulter, Brea, CA, USA) for 1 h and visualized using LSM5 PASCAL (Carl Zeiss, Oberkochen, Germany). We observed cells with ×400 magnification and presented the mean percentage LC3 puncta-positive or puncta >10 cells ±SEM in five different fields of vision. In each field, approximately 30 cells were analyzed.

Cell proliferation assay. A total of 5×10^3 cells per well were seeded and incubated in a 96-well plate for 24 h. They were then treated with drugs and further cultured until 48 h at 37°C. Cell proliferation assay were performed with a Cell Counting Kit-8 (Dojin Laboratories, Kumamoto, Japan) as described previously.[24]

Cell cycle analysis by FACS. A total of 1.5×10^4 cells per plate were seeded and incubated in a 6-cm culture plate for 24 h. They were further incubated in the presence of drugs for 48 h. These cells were collected and FACS was performed as described previously.[26]

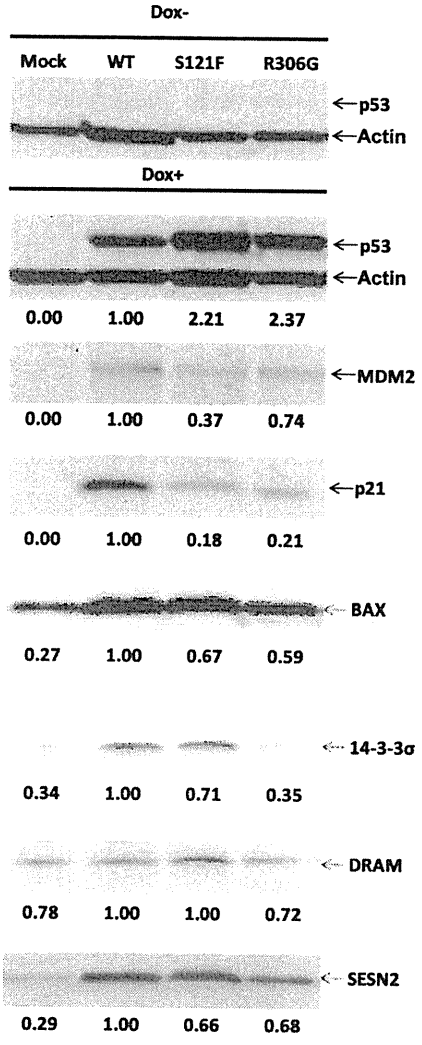

Fig. 1. Induction of p53 and its downstream genes by Dox. After 24-h incubation with or without Dox (10 ng/mL), expression levels of p53, MDM2, p21WAF1, BAX, 14-3-3sigma, DRAM and Sesn2 were analyzed by western blotting. β-Actin was used as an internal control. Numbers indicated under the top panel are the expression levels of p53/β-actin (expression level of wild-type [WT] p53/expression level of β-actin = 1.00). Numbers indicated under the other panels are the expression levels of downstream genes/β-actin (the product induced by WT p53/WT p53 = 1.00).

Results

Characterization of established cell lines. As shown in Figure 1, the established cell lines expressed p53 in a Dox-dependent manner, but with different expression levels, and the expression level of WT p53 was lower than those of S121F and R306G. To determine the transcriptional activities of the expressed p53, we also performed western blotting of well-known p53 downstream gene products. Although the WT p53 expression level was lower than that of MT p53s, all the examined downstream gene products were highly induced by WT p53. DRAM and SESN2 are p53 downstream genes that induce autophagy and they also upregulated in our system.

Immunofluorescence analysis revealed that WT p53 and S121F mutants were mainly localized in the nucleus, and R306G mutants were mainly localized in the cytosol (Fig. 2a). To quantify the distribution of p53 protein, we performed subcellular fractionation to divide the cells into nuclear and cytosolic fractions for immunoblotting. As shown in Figure 2(b,c), more than 80% of WT p53 and S121F mutants were localized in the nucleus, while approximately 80% of R306G was localized in the cytosol.

We then performed a cell proliferation assay (Fig. 3a). At 48 h after Dox treatments, cell proliferation was inhibited by WT p53 expression and the total cell number was equal to that at the start. Cell proliferation was also inhibited by S121F expression, but the total cell number decreased markedly compared with that seen with WT p53 expression. R306G expression inhibited cell proliferation, but its effect was weak in comparison to that exerted by WT p53 and S121F.

doi: 10.1111/j.1349-7006.2011.01857.x

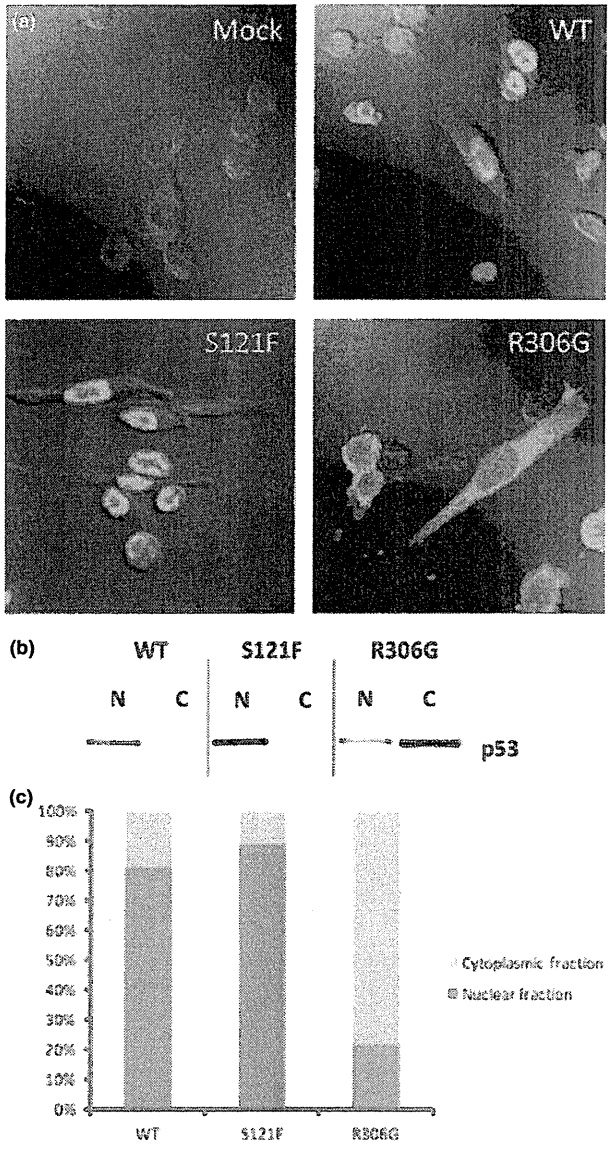

Fig. 2. Analysis of p53 localization. (a) Immunostaining of p53. (b) Western blotting of nuclear and cytosolic fractions. (c) Quantification of the p53 expression level in nuclear and cytosolic fractions analyzed in (b).

Finally, we examined the effect of WT and MT p53 expression on the cell cycle by FACS (Fig. 3b). The sub-G1 fraction was prominently increasing in S121F, followed by WT p53 and R306G. On the other hand, the proportion of the S-phase fraction was decreased by WT p53 and S121F expression, but not by R306G expression. These results showed that WT p53 had cell cycle arrest-inducing as well as apoptosis-inducing activity, while S121F tended to induce apoptosis rather than cell cycle arrest.

Analysis of autophagy inducible abilities of WT and MT p53. Autophagy is induced under nutrient deprivation, and stimulated autophagy was observed by increasing LC3 puncta-positive cells and LC3-I to LC3-II conversion.[27]

Thus, we examined whether autophagy was stimulated in established cell lines under serum-starved conditions. As shown in Figure S1, LC3 puncta-positive cells were increased under serum-starved conditions. LC3-I to LC3-II conversion was also accelerated in all cell lines (Fig. S2); thus, autophagy was detected in SF126 cells under serum-starved conditions.

We then examined whether WT and MT p53 expression stimulates autophagy even under serum-rich conditions. LC3 puncta-positive and puncta >10 cells accumulated in all Dox-treated WT clones, and even MT clones, but not in mock clones (Fig. 4). In the same way, LC3-I to LC3-II conversion was also accelerated when WT and MT p53 were expressed (Fig. 5 lanes 1 and 5).

These data showed that WT and MT p53 expression stimulates autophagy in established cells.

Contribution of autophagy to apoptosis, cell cycle arrest and the inhibition of cell proliferation induced by WT and MT p53. To examine the p53-induced autophagy influence on apoptosis, cell cycle arrest and inhibition of cell proliferation we analyzed them in the established cell lines under the p53 expression conditions using the autophagy inhibitor 3MA or pan-caspase inhibitor VAD.

Adding 3MA, LC3-I to II conversions were decreased in the WT and MT p53 clones (Fig. 5 lanes 5 and 6), but it was rather slightly increased in the mock clones. The number of LC3 puncta-positive cells in WT and MT p53 expressed cells also decreased by adding 3MA (Fig. S3). In contrast to 3MA, VAD did not change LC3-I to II conversions and the number of LC3 puncta-positive cells (Fig. 5 lanes 5 and 7, Fig. S3). These data showed that 3MA block the WT and MT p53-induced autophagy. We then analyzed if the characters of these clones induced by WT and MT p53 change under the blocking autophagy by 3MA.

In mock clones with Dox, adding 3MA or VAD did not increase the sub-G1 fraction, but the S-phase fraction was decreased and cell proliferation was blocked by the 3MA treatments (Fig. 6a,b lanes 5–7). Similar results were obtained from other clones without p53 expression (Fig. 6c–h lanes 1–3). These data showed that under the serum-rich and without p53 condition, 3MA did not influence the autophagy status, but induced cell cycle arrest and resulted in inhibiting cell proliferation, without apoptosis.

In contrast to the mock clone, adding 3MA slightly decreased the sub-G1 fraction and increased the S-fraction on the WT p53 clone (Fig. 6c lanes 5 and 6), thus attenuating the inhibition of cell proliferation (Fig. 6d lanes 5 and 6). Thus, blocking autophagy by 3MA under WT p53 expression conditions results in antagonizing p53 functions such as increasing sub-G1 fraction, cell cycle arrest (S phase) and inhibition of cell proliferation. VAD treatment slightly decreased the sub-G1 fraction, and the proportion of the S-phase fraction did not change (Fig. 6c lanes 5 and 7); however, the inhibition of cell proliferation was attenuated (Fig. 6d lanes 5 and 7). To reveal that increased sub-G1 fraction induced by WT p53 represents the increasing apoptosis fraction, we measured the activity of caspase-3/7 activities (Fig. S4). VAD treatment blocks the pro-caspase activities completely, but 3MA treatments did not influence caspase activities in WT, but rather increased it. On the other side, 3MA treatment increased the total cell number (Fig. 6d lanes 5 and 6). We also found that DRAM knockdown, one of the key molecules of p53-induced autophagy, also increased the total cell number (data not shown). These data indicate that p53-induced autophagy is one of the reasons for the amount of cell death.

On the other hand, apoptosis induced by S121F expression was not rescued by 3MA and the S-phase fraction was slightly decreased (Fig. 6e lanes 5 and 6). The inhibition of cell proliferation was slightly attenuated, but the total cell number was decreased compared with that seen before S121F expression by the 3MA treatment (Fig. 6f lanes 5 and 6). VAD treatment also had a minimal effect on apotosis and inhibition of cell proliferation induced S121F (Fig. 6e,f lanes 5 and 7). VAD treatment strongly blocked the caspase-3/7 activities in S121F cell lines

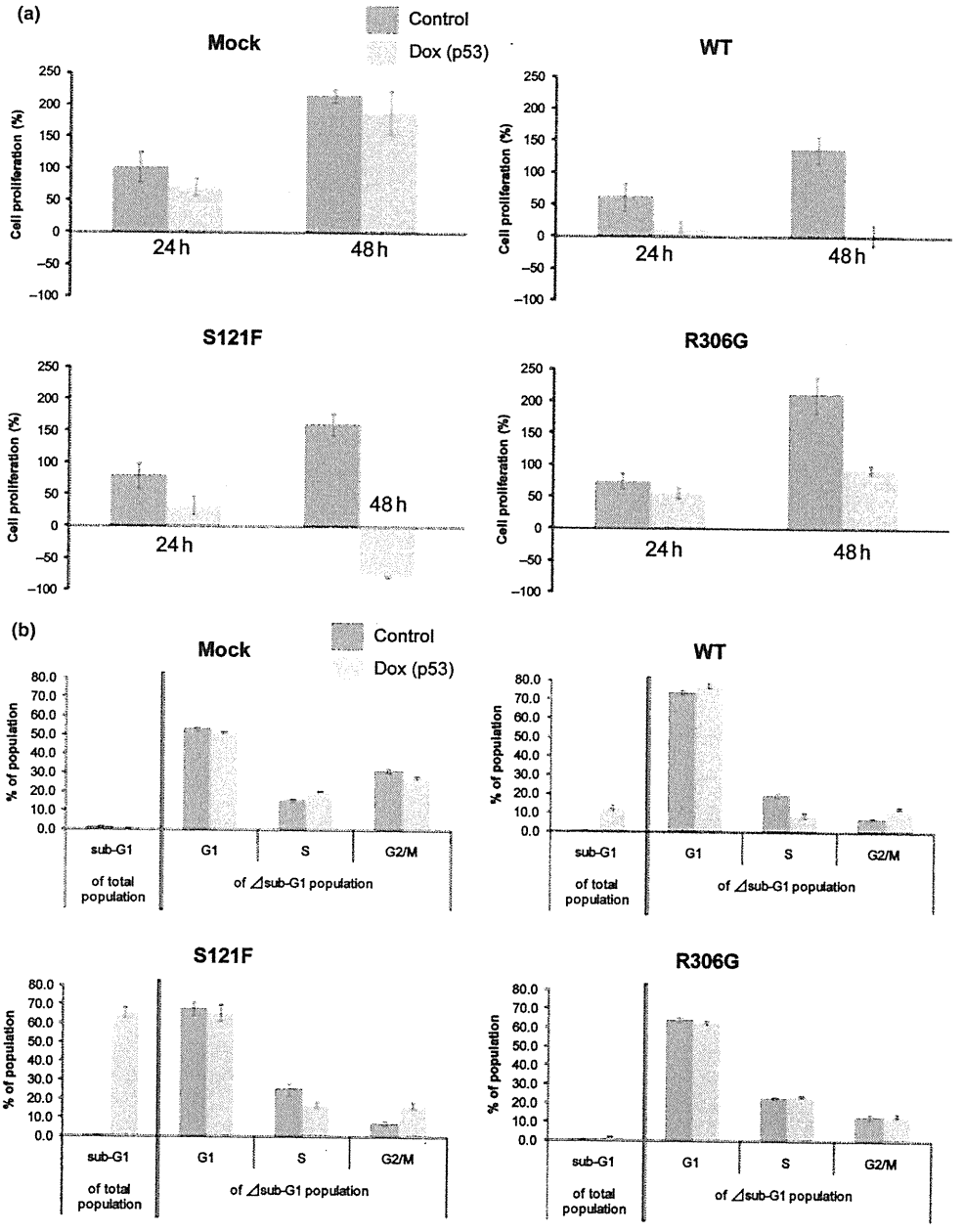

Fig. 3. Cell proliferation assay and cell cycle analysis of established cell lines. (a) Cell proliferation assay of each clone. The cell viability just before treatment was 0%. Values shown are mean ± SD (n = 3). (b) DNA histogram of each clone with or without p53 expression. After 48-h incubation with or without Dox (10 ng/mL), cells were harvested and analyzed by FACS. Values shown are mean ± SD (n = 3). Value of the sub-G1 fraction is a portion of the total population, and values of G1, S and G2/M fractions were portions of the population excluding the sub-G1 fraction.

the same as WT, while the subG1 fraction did not decrease (Fig. 6e). We consider that WT p53 and especially S121F induce caspase-independent apoptosis[28] and the subG1 fraction was composed of caspase-independent apoptosis and caspase-dependent apoptosis.

Finally, we examined whether 3MA and VAD treatments influence the R306G phenotype. Treatment with 3MA did not change the sub-G1 fraction or the proportion of the fraction in each cell cycle phase (Fig. 6g lanes 5 and 6). Furthermore, inhibition of cell proliferation was slightly attenuated (Fig. 6h lanes 5 and 6). VAD also did not change the sub-G1 fraction, the proportion of the fraction in each cell cycle phase and the inhibition of cell proliferation (Fig. 6g,h lanes 5 and 7).

These data indicated that 3MA also inhibited R306G-induced autophagy as well as other WT p53 and S121F, but blocking autophagy did not influence its phenotype.

All the data are summarized in Figure 7 and Table 1.

Discussion

Dual contribution of apoptosis and autophagic cell death to p53-dependent cell death. Previous studies have reported that

doi: 10.1111/j.1349-7006.2011.01857.x

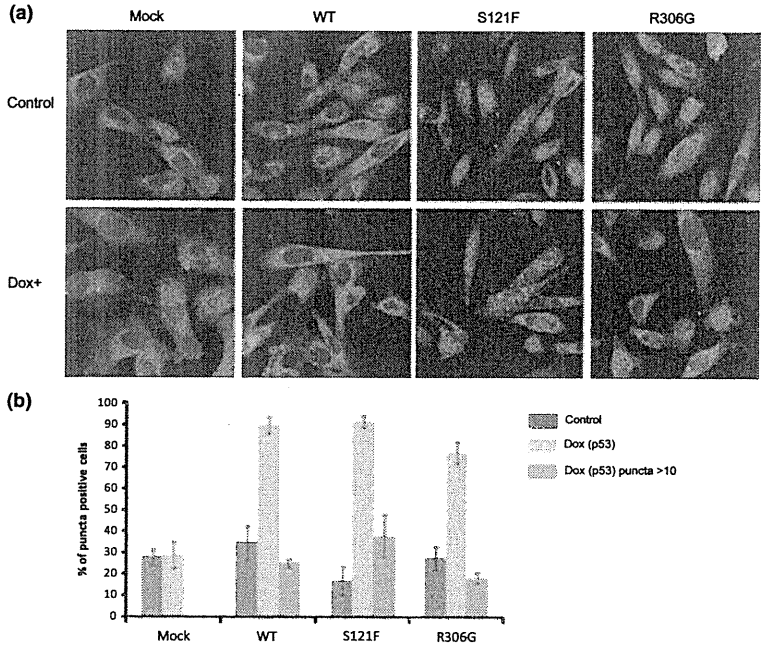

Fig. 4. LC3 puncta induced by p53. (a) Cells were incubated under serum-rich conditions, and 18 h after adding Dox (10 ng/mL), cells were harvested, fixed and immunostained. (b) Puncta-positive cells and puncta >10 cells were counted. Five-field vision (more than 30 cells/one field) was used for scanning and the percentage of puncta-positive cells was calculated. Values shown are average ± SD (n = 5).

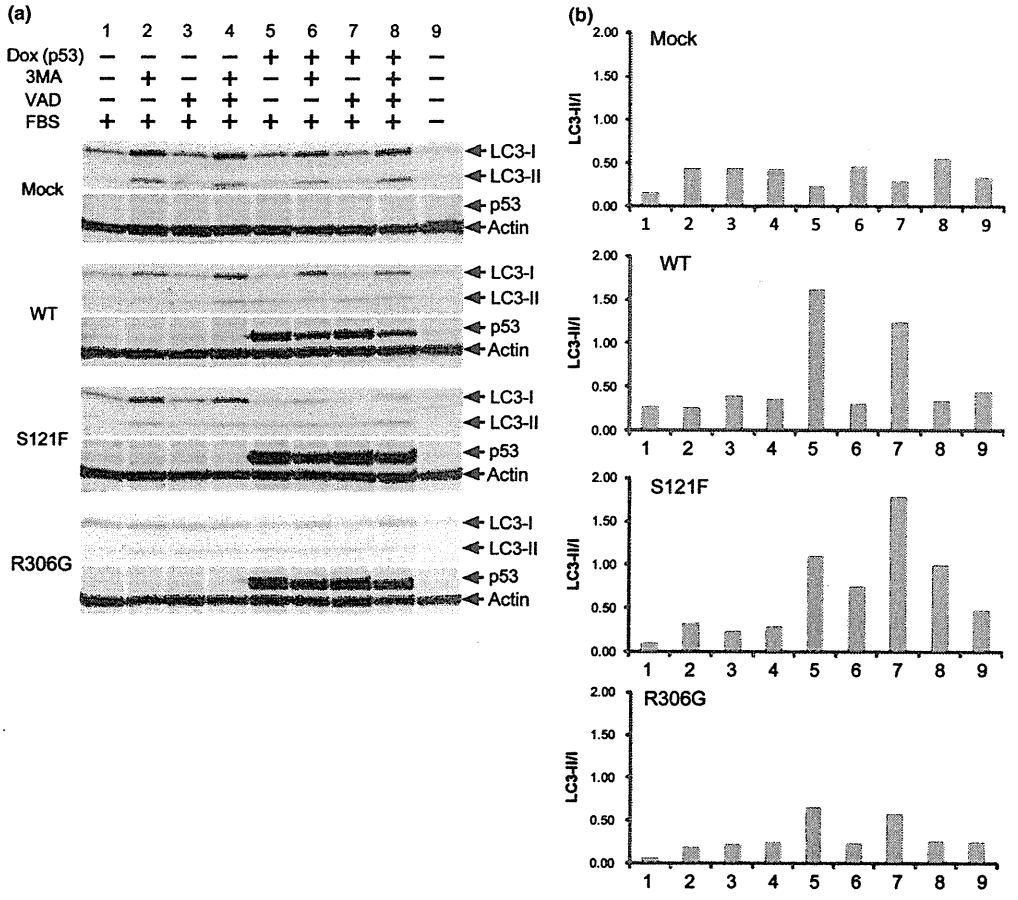

Fig. 5. Immunoblotting of LC3 with 3MA or/and VAD treatment on the established cell lines. (a) Cells were treated with Dox (10 ng/mL) and/or 3MA (6 mM) and/or VAD (10 μM), or starvation (FBS−), and then incubated for 24 h and harvested. Whole cell extracts were immunoblotted by LC3. β-Actin was used as an internal control. (b) Intensities of LC3-I and LC3-II bands were quantified and LC3-II/LC3-I is represented.

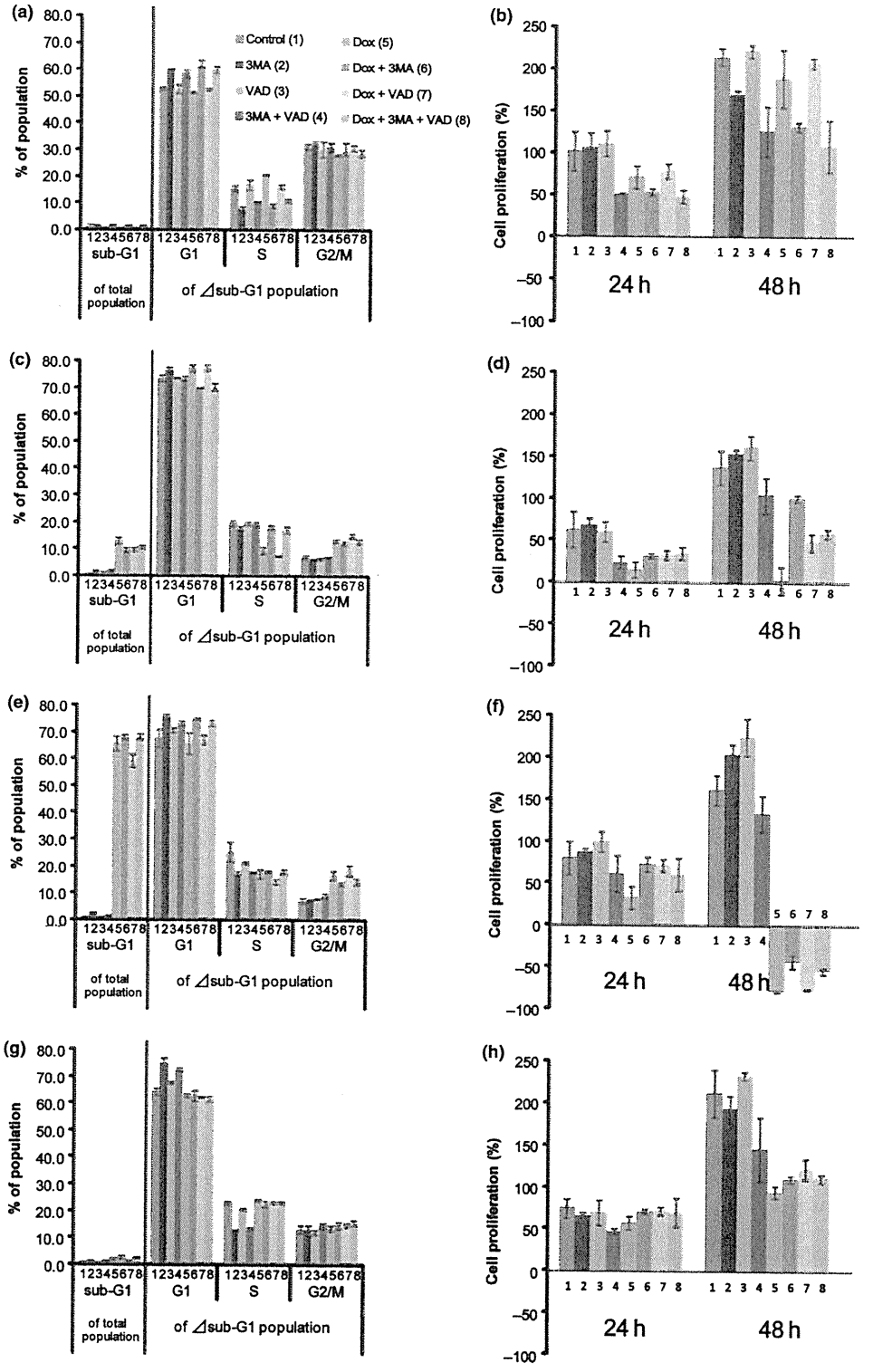

Fig. 6. Analysis of the proportion of each cell cycle phase and cell proliferation assay in established cell lines with 3MA and VAD treatments. FACS analysis (a, Mock; c, wild-type [WT]; e, S121F; g, R306G) and cell proliferation assay (b, Mock; d, WT; f, S121F; h, R306G) with or without Dox, 3MA and VAD treatments. Values shown are average ± SD (n = 3). Value of the sub-G1 fraction is a portion of the total population, and values of G1, S and G2/M fractions are portions of the population excluding the sub-G1 fraction. The cell viability just before treatment was 0%.

doi: 10.1111/j.1349-7006.2011.01857.x

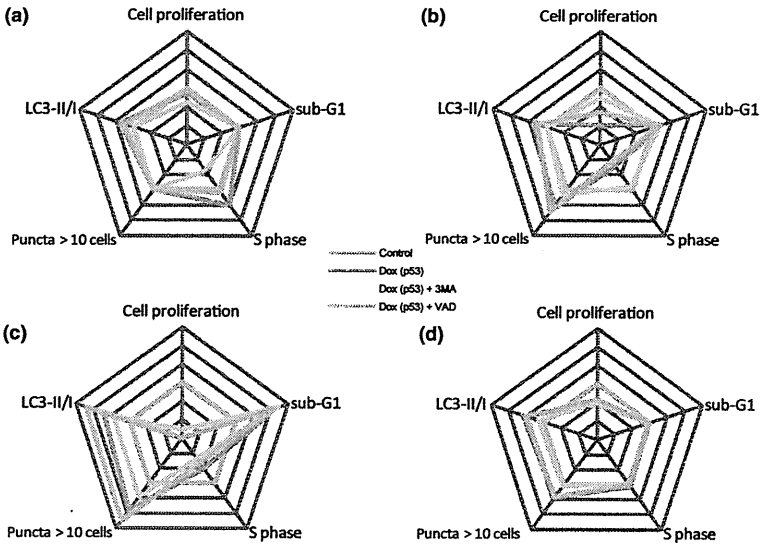

Fig. 7. Effects of p53 induction and apoptosis or autophagy inhibition on each clone. Values in Table 1 were normalized by each control value and illustrated in a radar chart. (a) Mock; (b) wild-type [WT]; (c) S121F; (d) R306G.

Table 1. The summary of character of established cell lines treating with pan-caspase and autophagy inhibitors

	Control	Dox (p53)	Dox (p53) + 3MA	Dox (p53) + VAD
Mock				
Cell proliferation (%)	215 ± 11.4†	189 ± 38.4†	132 ± 5.8†	209 ± 6.9†
Sub-G1 (%)	1.1 ± 0.62†	0.5 ± 0.00†	1.4 ± 0.11†	0.5 ± 0.17†
S phase (%)	15.5 ± 1.19†	20.6 ± 0.20†	9.3 ± 0.66†	16.3 ± 1.09†
Puncta-positive cells (%) (>10)	27.9 ± 3.44† (0.0)	29.0 ± 5.57† (0.0)	29.1 ± 14.53† (0.0)	32.4 ± 9.50† (0.0)
LC3-II/I	0.155	0.241	0.464	0.298
WT p53				
Cell proliferation (%)	137 ± 22.8†	3 ± 17.7†	100 ± 4.7†	48 ± 11.1†
Sub-G1 (%)	0.7 ± 0.00†	12.8 ± 1.54†	9.5 ± 0.82†	9.7 ± 0.53†
S phase (%)	19.4 ± 1.41†	9.4 ± 1.31†	17.9 ± 0.91†	7.6 ± 0.24†
Puncta-positive cells (%) (>10)	34.8 ± 7.07† (0.0)	90.0 ± 3.37† (25.2 ± 1.90†)	75.2 ± 3.49† (7.6 ± 2.69†)	93.4 ± 4.06† (31.5 ± 6.55†)
LC3-II/I	0.266	1.611	0.305	1.242
S121F				
Cell proliferation (%)	161 ± 19.6†	−79 ± 1.4†	−44 ± 9.1†	−77 ± 0.9†
Sub-G1 (%)	0.8 ± 0.13†	65.6 ± 2.94†	68.1 ± 1.05†	59.2 ± 2.66†
S phase (%)	25.3 ± 3.99†	17.1 ± 1.79†	11.6 ± 0.58†	14.1 ± 0.92†
Puncta-positive cells (%) (>10)	16.8 ± 5.67† (0.0)	91.7 ± 2.33† (37.7 ± 8.68†)	82.9 ± 4.26† (19.1 ± 2.29†)	96.8 ± 2.25† (52.3 ± 9.17†)
LC3-II/I	0.096	1.099	0.746	1.79
R306G				
Cell proliferation (%)	212 ± 32.1†	94 ± 7.9†	109 ± 4.3†	122 ± 13.4†
Sub-G1 (%)	0.7 ± 0.11†	1.9 ± 0.41†	2.5 ± 0.53†	1.3 ± 0.17†
S phase (%)	22.9 ± 0.62†	23.8 ± 0.59†	22.5 ± 1.14†	22.9 ± 0.46†
Puncta-positive cells (%) (>10)	27.4 ± 4.76† (0.0)	77.1 ± 4.42† (18.1 ± 2.29†)	32.3 ± 8.06† (2.2 ± 3.53†)	82.3 ± 6.86† (18.0 ± 3.92†)
LC3-II/I	0.070	0.654	0.238	0.581

†Values shown are mean ± SD (95% CI).

overexpression of WT p53 induces both apoptosis and autophagy.[15,29–31] However, it is still unclear whether the autophagy induced by p53 contributed to p53-dependent cell death. In this study, we demonstrated that conditional overexpression of WT p53 in the human glioblastoma cell line SF126 induced both apoptosis and cell death by autophagy, and consequently inhibited cell proliferation. Inhibition of p53-induced autophagy by 3MA released cell cycle arrest and inhibition of cell proliferation but slightly inhibited apoptosis. Inhibition of p53-induced apoptosis by VAD released inhibition of cell proliferation without affecting autophagy. The degree of recovery of cell proliferation by 3MA was higher than that of VAD, indicating that contribution of autophagic cell death was important to p53-dependent cell death as well as apoptosis. We also examined whether the autophagy was induced by p53 expression using *TP53*-null SaOS2 cells, but under the p53 expressed conditions in SaOS2 cells, the autophagy was not induced (unpublished data, Y.S.). The reason for this remains unclear, but the pathway of p53-induced autophagy may be uncontrollable in SaOS2 cells.

These results suggest that activation of p53-induced autophagy, as well as activation of apoptosis, is a potential therapeutic target for cancer treatment in some types of tumors with WT p53. But it remained to dissolve that precise molecular mechanism of p53 inducing autophagic cell death.

Separation of p53-induced autophagy and apoptosis pathways. Compared with WT p53, S121F demonstrated a stronger ability to induce cell death but retained a similar ability to

induce autophagy. When S121F-induced autophagy was inhibited by 3MA, it did not affect caspase-dependent apoptosis and did not release inhibition of cell proliferation. These results suggest that a p53-induced autophagy pathway is separable from a p53-induced caspase-dependent apoptosis pathway.

One possible explanation is that the induction of apoptosis and autophagy is independently regulated by distinct p53-downstream genes, and the genes are differentially transactivated by WT p53 and by S121F. For example, S121F might preferentially transactivate pro-apoptotic genes. However, we have previously shown a lack of correlation between p53-dependent transcriptional activity of downstream genes for apoptosis and cell cycle arrest and the ability to induce apoptosis among 179 mutant p53 including S121F.[26] In that study, there was no correlation between the ability to induce apoptosis and p53-downstream pro-apoptotic genes among WT p53 and S121F. Because the induction of autophagy was similar among WT p53, S121F and R306G, induction of p53-dependent autophagy may not be correlated with p53-dependent transactivation of known downstream genes for apoptosis and cell cycle arrest.

Whether p53-induced autophagy depends on the transactivation function of p53 needs to be elucidated by further studies including identification of new p53-downstream genes related to autophagy and analysis of the transactivation-independent mechanism of p53-induced autophagy.

Cytoplasmic p53 and induction of apoptosis and autophagy. Among common p53 polymorphisms R72 and P72, the R72 variant has a stronger ability to induce apoptosis and a greater ability to localize to the cytoplasm (especially to mitochondria) of cells than the P72 variant.[19] Because R306G mainly locates cytoplasm, we speculate that it may possess a stronger ability to induce apoptosis than WT p53. Unexpectedly, induction of apoptosis by R306G was only slight and was much weaker than those of WT p53 and S121F. It has been shown that apoptosis by cytoplasmic p53 needs collaboration of PUMA and BAX, p53-downstream proteins, in mitochondria.[10] We speculate that R306G may not induce efficient apoptosis because it does not efficiently transactivate downstream genes.

Recently, cytoplasmic p53 has been shown to inhibit autophagy.[20] However, in this study, cytoplasmic mutant R306G failed to inhibit autophagy, but rather slightly induced it. There are at least two speculations explaining the distinct observations. First, cytoplasmic R306G partially inhibits autophagy induced by nuclear R306G, and the observation is the sum total. Second, as in the case of apoptosis, autophagy by cytoplasmic p53 needs collaboration of some p53-downstream proteins, and R306G may not induce the downstream genes.

In conclusion, we demonstrated that in the human glioblastoma cell line SF126, inhibition of cell proliferation by WT p53 consisted of apoptosis and autophagic cell death, and that the contribution of autophagic cell death to p53-dependent cell death was stronger than that of apoptosis. We also demonstrated that the p53-induced autophagy pathway was independent from the p53-induced apoptosis pathway.

Acknowledgments

The authors thank Eri Yokota for her technical assistance. This study was supported by grants-in-aid from the Ministry of Education, Culture, Sports, Science and Technology (12217010 and 17015002), and the Gonryo Medical Foundation to C.I. and Sapporo Bioscience Foundation to S.K.

References

1 Sawyers C. Targeted cancer therapy. *Nature* 2004; **432**: 294–7.
2 Tan ML, Ooi JP, Ismail N, Moad AI, Muhammad TS. Programmed cell death pathways and current antitumor targets. *Pharm Res* 2009; **26**: 1547–60.
3 Taylor RC, Cullen SP, Martin SJ. Apoptosis: controlled demolition at the cellular level. *Nat Rev Mol Cell Biol* 2008; **9**: 231–41.
4 Maiuri MC, Zalckvar E, Kimchi A, Kroemer G. Self-eating and self-killing: crosstalk between autophagy and apoptosis. *Nat Rev Mol Cell Biol* 2007; **8**: 741–52.
5 Debnath J, Baehrecke EH, Kroemer G. Does autophagy contribute to cell death? *Autophagy* 2005; **1**: 66–74.
6 Levine B, Yuan J. Autophagy in cell death: an innocent convict? *J Clin Invest* 2005; **115**: 2679–88.
7 Kroemer G, Levine B. Autophagic cell death: the story of a misnomer. *Nat Rev Mol Cell Biol* 2008; **9**: 1004–10.
8 Qu X, Yu J, Bhagat G *et al.* Promotion of tumorigenesis by heterozygous disruption of the *beclin-1* autophagy gene. *J Clin Invest* 2003; **112**: 1809–20.
9 Yue Z, Jin S, Yang C, Levine AJ, Heintz N. *Beclin-1*, an autophagy gene essential for early embryonic development, is a haploinsufficient tumor suppressor. *Proc Natl Acad Sci U S A* 2003; **100**: 15077–82.
10 Green DR, Kroemer G. Cytoplasmic functions of the tumour suppressor p53. *Nature* 2009; **458**: 1127–30.
11 Harris SL, Levine AJ. The p53 pathway: positive and negative feedback loops. *Oncogene* 2005; **24**: 2899–908.
12 Miyashita T, Reed JC. Tumor suppressor p53 is a direct transcriptional activator of the human bax gene. *Cell* 1995; **80**: 293–9.
13 Oda K, Arakawa H, Tanaka T *et al.* p53AIP1, a potential mediator of p53-dependent apoptosis, and its regulation by Ser-46-phosphorylated p53. *Cell* 2000; **102**: 849–62.
14 Yu J, Zhang L, Hwang PM, Kinzler KW, Vogelstein B. PUMA induces the rapid apoptosis of colorectal cancer cells. *Mol Cell* 2001; **7**: 673–82.
15 Crighton D, Wilkinson S, O'Prey J *et al.* DRAM, a p53-induced modulator of autophagy, is critical for apoptosis. *Cell* 2006; **126**: 121–34.
16 Maiuri MC, Malik SA, Morselli E *et al.* Stimulation of autophagy by the p53 target gene *Sestrin 2*. *Cell Cycle* 2009; **8**: 1571–6.
17 Budanov AV, Karin M. p53 target genes *sestrin 1* and *sestrin 2* connect genotoxic stress and mTOR signaling. *Cell* 2008; **134**: 451–60.
18 Chipuk JE, Kuwana T, Bouchier-Hayes L *et al.* Direct activation of Bax by p53 mediates mitochondrial membrane permeabilization and apoptosis. *Science* 2004; **303**: 1010–4.
19 Dumont P, Leu JI, Della Pietra AC III, George DL, Murphy M. The codon 72 polymorphic variants of p53 have markedly different apoptotic potential. *Nat Genet* 2003; **33**: 357–65.
20 Tasdemir E, Maiuri MC, Galluzzi L *et al.* Regulation of autophagy by cytoplasmic p53. *Nat Cell Biol* 2008; **10**: 676–87.
21 Morselli E, Tasdemir E, Maiuri MC *et al.* Mutant p53 protein localized in the cytoplasm inhibits autophagy. *Cell Cycle* 2008; **7**: 3056–61.
22 Saller E, Tom E, Brunori M *et al.* Increased apoptosis induction by 121F mutant p53. *EMBO J* 1999; **18**: 4424–37.
23 Liang SH, Clarke MF. A bipartite nuclear localization signal is required for p53 nuclear import regulated by a carboxyl-terminal domain. *J Biol Chem* 1999; **274**: 32699–703.
24 Watanabe G, Kato S, Nakata H, Ishida T, Ohuchi N, Ishioka C. alphaB-crystallin: a novel p53-target gene required for p53-dependent apoptosis. *Cancer Sci* 2009; **100**: 2368–75.
25 Kato S, Han SY, Liu W *et al.* Understanding the function-structure and function-mutation relationships of p53 tumor suppressor protein by high-resolution missense mutation analysis. *Proc Natl Acad Sci U S A* 2003; **100**: 8424–9.
26 Kakudo Y, Shibata H, Otsuka K, Kato S, Ishioka C. Lack of correlation between p53-dependent transcriptional activity and the ability to induce apoptosis among 179 mutant p53s. *Cancer Res* 2005; **65**: 2108–14.
27 Klionsky DJ, Abeliovich H, Agostinis P *et al.* Guidelines for the use and interpretation of assays for monitoring autophagy in higher eukaryotes. *Autophagy* 2008; **4**: 151–75.
28 Bröker LE, Kruyt FA, Giaccone G. Cell death independent of caspases: a review. *Clin Cancer Res* 2005; **11**: 3155–62.
29 Abida WM, Gu W. p53-Dependent and p53-independent activation of autophagy by ARF. *Cancer Res* 2008; **68**: 352–7.
30 Zeng X, Yan T, Schupp JE, Seo Y, Kinsella TJ. DNA mismatch repair initiates 6-thioguanine-induced autophagy through p53 activation in human tumor cells. *Clin Cancer Res* 2007; **13**: 1315–21.
31 Feng Z, Zhang H, Levine AJ, Jin S. The coordinate regulation of the p53 and mTOR pathways in cells. *Proc Natl Acad Sci U S A* 2005; **102**: 8204–9.

doi: 10.1111/j.1349-7006.2011.01857.x

Supporting Information

Additional Supporting Information may be found in the online version of this article:

Fig. S1. LC3 puncta induced by serum starvation.

Fig. S2. LC3-I to LC3-II conversion occurred under serum starvation.

Fig. S3. Quantification of LC3 puncta cells in each cell line with Dox, 3MA and VAD treatments.

Fig. S4. Quantification of caspase-3/7 activities shown in Figure 6.

Please note: Wiley-Blackwell are not responsible for the content or functionality of any supporting materials supplied by the authors. Any queries (other than missing material) should be directed to the corresponding author for the article.

Induction of apoptosis by cytoplasmically localized wild-type p53 and the S121F mutant super p53

KATSUHIRO YASUDA, SHUNSUKE KATO, YASUHIRO SAKAMOTO, GOU WATANABE, SATSUKI MASHIKO, ATSUKO SATO, YUICHI KAKUDO and CHIKASHI ISHIOKA

Department of Clinical Oncology, Institute of Development, Aging and Cancer, Tohoku University, Sendai, Miyagi 980-8575, Japan

Received February 13, 2012; Accepted February 21, 2012

DOI: 10.3892/ol.2012.624

Abstract. After DNA damage, p53 is accumulated in the nucleus and transactivates downstream genes and induces apoptosis. There are two pathways in p53-dependent apoptosis, the transactivation-dependent and -independent pathway. In this study, we constructed p53-inducible glioblastoma cell lines and analyzed them for the induction of apoptosis and transactivation of p53-downstream genes after the nuclear or cytoplasmic expression of p53. To sequester p53 in the cytoplasm, we used p53 mutant with arginine to glycine substitution at residue 306 (R306G). Wild-type p53 retained the ability to arrest the cell cycle, and a p53 mutant with serine to phenylalanine substitution at residue 121 (S121F), which has a strong ability to induce apoptosis, retained this ability even when both the wild-type and p53 and S121F mutant were exclusively sequestered from the nucleus into the cytoplasm. Notably, cytoplasmically sequestered wild-type p53 and S121F mutant transactivated the downstream genes with distinct expression profiles, and the strong apoptotic ability of S121F was not associated with its transactivation activity. These results underscore the existence of transactivation-independent apoptosis and cytoplasmic function of p53.

Introduction

TP53 tumor suppressor gene is one of the most commonly mutated genes in human neoplasia, and approximately 80% of these mutations are missense mutations (1,2). The gene product, p53 protein, is a nuclear transcriptional activator that is activated by post-translational modification, including phosphorylation and acetylation, in response to DNA-damaging stresses. Activated p53 is stabilized, accumulates in the nucleus and binds to p53-responsive elements (p53REs) in the promoter region of p53-downstream genes (3). Transactivation of these genes, including *p21WAF1*, *MDM2*, *p53AIP1*, *BAX*, *NOXA* and *PUMA*, results in cell cycle arrest and apoptosis.

Most p53 mutants with a single amino acid substitution found in human neoplasm lose the ability to bind to p53REs, and this functional defect is thought to be one of the most important oncogenic events caused by *TP53* mutation (4). Therefore, the translocation of p53 into the nucleus is crucial for normal p53 function. Cytoplasmic sequestration of wild-type p53 was observed in undifferentiated neuroblastoma, breast cancer, retinoblastoma, colorectal carcinoma and glioblastoma cells (5-7). In all these cells, wild-type p53 is inactivated since it is retained in the cytoplasm. Although the precise mechanism underlying the cytoplasmic sequestration remains unclear, several molecular mechanisms have been proposed: i) a mutation in the bipartite sequence of p53 (residues 305 and 306) (8) or a truncated mutation of the nuclear localization motif receptor protein importin-α (9); ii) hyperactive nuclear export by an MDM2-dependent pathway (10); and iii) overexpression of cytoplasmic tethering proteins, such as mortalin (11), cullin 7 (12) and PARC (13). The mutations in the bipartite sequence have been analyzed comprehensively, and these mutants were shown to lose transactivation activity in a yeast functional assay (14).

In contrast to tumor-derived loss-of-function p53 mutants, other types of p53 mutants (super p53s) have a stronger ability to induce apoptosis than wild-type p53. Among these, a p53 mutant with a serine to phenylalanine substitution at residue 121 (S121F) has a distinct affinity to bind p53REs from wild-type p53 (15). S121F induces a more potent apoptosis than wild-type p53 in mammalian cell lines. The transcriptional activity of S121F for downstream genes, however, is less efficient than that of wild-type p53 (16). In addition, different expression profiles among super p53s have been reported (17). These results suggest that transactivation-independent cytoplasmic activity occurs in p53-dependent apoptosis and that S121F may be a diverged mutant with enhanced cytoplasmic activity.

To test this hypothesis, we expressed wild-type and S121F p53 in the nucleus or cytoplasm of p53-null SF126 glioblastoma cells using a p53 mutant with an arginine to glycine substitution at residue 306 (R306G), and analyzed them for induction of apoptosis and transactivation of p53-downstream genes following the p53 induction.

Correspondence to: Dr Chikashi Ishioka, Department of Clinical Oncology, Institute of Development, Aging and Cancer, Tohoku University, Sendai, Miyagi 980-8575, Japan
E-mail: chikashi@idac.tohoku.ac.jp

Key words: p53, tumor suppressor, apoptosis, subcellular localization

Materials and methods

Construction of stable SF126 glioblastoma cell lines. The plasmids pCR259-WTp53, pCR259-S121F and pCR259-R306G were previously constructed (14). pCR259-S121F-R306G was constructed by inserting a small fragment of pCR259-R306G into the *Bsu*36I/*Eag*I site of pCR259-S121F. The small *Nhe*I/*Eag*I fragments of the four pCR259-based plasmids were inserted into the *Nhe*I/*Not*I site of pcDNA5/TON (Invitrogen, Carlsbad, CA, USA). The resulting plasmids were designated pcDNA5/TON-WTp53, pcDNA5/TON-S121F, pcDNA5/TON-R306G and pcDNA5/TON-S121F-R306G, respectively. The stable SF126 cell lines expressing tetracycline-inducible p53 were constructed according to the protocol described in the T-Rex™ System (Invitrogen) using the four pcDNA5/TON-based plasmids. For each category, several stable clones were selected by hygromycin B (100 μg/ml) and two independent stable clones were used.

Western blot analysis. The cell lines were harvested and the cells were resuspended in lysis buffer containing 50 mM Tris-HCl, pH 8.0, 150 mM NaCl, 5 mM EDTA and 1% protease inhibitor cocktail (Sigma-Aldrich, St. Louis, MO, USA). Cell lysates were centrifuged for 10 min at 4°C. The supernatants were resolved by SDS-PAGE and transferred to PVDF membranes. The membranes were incubated with anti-p53 (FL-393; Santa Cruz Biotechnology, Santa Cruz, CA, USA) and mouse anti-actin (Sigma-Aldrich), followed by incubation with goat anti-rabbit Alexa Fluor 680 IgG (Invitrogen) and goat anti-mouse IR Dye 800 CW IgG (Rockland, Gilbertsville, PA, USA). Expression of both p53 and β-actin was visualized using an Odyssey Infrated Imaging System (LI-COR, Lincoln, NE, USA).

Immunofluorescent analysis. Each cell line was cultured on poly-D lysine-coated Lab-Tek Chamber Slides™ (Nalge Nunc, Rochester, NY, USA) until 70% confluence was achieved. At 24 h after the addition of 10 ng/ml doxycycline or phosphate-buffered solution (PBS), the cells were fixed with acetone-methanol (1:1) and incubated for 20 min at -20°C. After washing with PBS and blocking with 5% non-fat milk in PBS containing 0.05% Tween-20 for 1 h, cells were incubated with FITC-conjugated mouse anti-p53 (DO-1 FITC; Santa Cruz Biotechnology, Santa Cruz, CA, USA) diluted at 1:500, stained with propidium iodide and then visualized on an LSM5 PASCAL (Carl Zeiss, Jena, Germany).

Cell proliferation assay. Cells ($4x10^3$) were seeded and incubated in a 96-well plate for 24 h. Doxycycline (10 ng/ml) or PBS was added to the medium and the cells were then cultured until 72 h at 37°C. At 0, 24, 48 and 72 h after the addition of doxycycline, 10 μl of the Cell Counting Kit-8 (Dojin Laboratories, Kumamoto, Japan) was added to each well and the cells were incubated for 2 h at 37°C. Absorbance at 490 nm was read with a microplate reader. Each data point is derived from triplicate experiments. The absorbance values at 24, 48 and 72 h were normalized by the value at 0 h.

Cell cycle analysis by fluorescence-activated cell sorting. Cells ($1x10^6$) were seeded and incubated in a 10-cm culture plate for 24 h, and then incubated in the presence of doxycycline (10 ng/ml). After 24 h, the cells were collected and stained with propidium iodide (50 μg/ml). The stained cells were filtered through 50-μm nylon mesh and analyzed using a Cytomics FC500 (Beckman Coulter, Miami, FL, USA). The subfraction of cells in each phase of the cell cycle was calculated using Multicycle software (Phoenix Flow Systems, San Diego, CA, USA). The average subfraction value of two independent cell lines was calculated.

Quantitative real-time PCR analysis. Total RNA was extracted from cells in the presence or absence of doxycycline using an RNeasy Mini kit (Qiagen, Gaithersburg, MD, USA). RNA (1 μg) was converted to cDNA using a High-Capacity cDNA Reverse Transcription kit (Applied Biosystems, Foster City, CA, USA) with random hexamers. TaqMan Gene Expression Assay was performed on the ABI 7500 real-time PCR System (Applied Biosystems) according to the manufacturer's protocol. Assay ID was as follows; GAPDH, Hs99999905_m1; ACTB (β-actin), Hs99999903_m1; MDM2, Hs01066938_m1; p21 (CDKN1A), Hs00355782_m1; BAX, Hs00180269_m1; NOXA (PMAIP1), Hs00560402_m1; PUMA (BBC3), Hs00248075_m1; and P53AIP1, Hs00223141_m1. The expression level of each p53 target gene was collected by either β-actin or GAPDH (data not shown). A relatively induced expression was measured as a ratio of the collected value of doxycycline presence against that of doxycycline absence. Two independent clones were analyzed, and the data were shown as a mean of four replicates with an error bar of standard deviation.

Results

Cytoplasmic sequestration of p53 by R306G mutation. To examine the cytoplasmic activity of wild-type p53 and the S121F mutant, we constructed a series of stable SF126 glioblastoma cell lines. These cells expressed wild-type p53, S121F, R306G or S121F-R306G double mutants in the presence of doxycycline (Fig. 1). To examine the cellular localization of doxycycline-induced p53, an immunofluorescent analysis was performed (Figs. 1 and 2). Both wild-type p53 and S121F localized mostly to the nucleus. In the presence of the R306G mutation in the same p53 molecule, wild-type p53 and S121F were exclusively sequestered from the nucleus to the cytoplasm. To quantify the degree of sequestration of p53, 100 cells of each cell clone were scored as having nuclear, cytoplasmic or both nuclear and cytoplasmic patterns (Fig. 2). Both wild-type and S121F thoroughly localized in the nucleus (>95% of cells), and no cell showed a cytoplasmic pattern. By contrast, both wild-type and S121F with R306G localized in the cytoplasm (>95%) or exhibited cytoplasmic and nuclear patterns. None of the cells expressing p53 exhibited any nuclear pattern. These results indicate that R306G sequestered p53 from the nucleus to the cytoplasm. This result is reasonable since R306G is a mutation in the bipartite sequence of p53 (residues 305 and 306) as described above.

Inhibition of cell proliferation by cytoplasmically localized wild-type p53 and S121F. To examine the effect of cytoplasmically localized wild-type p53 and the S121F mutant on cell proliferation, we cultured two independent cell lines for each

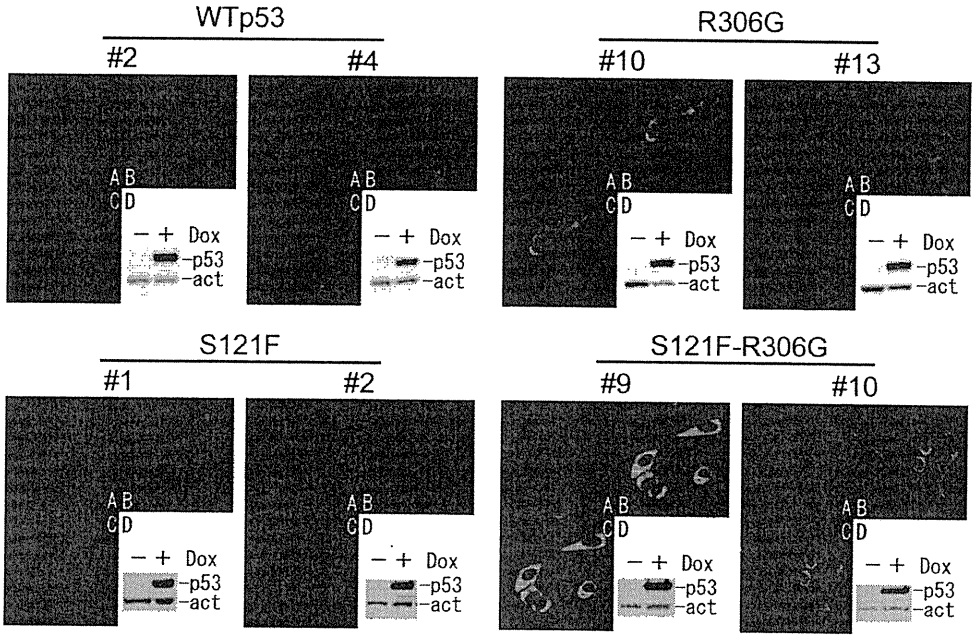

Figure 1. Inducible expression and subcellular localization of p53. Two independent clones in each category were analyzed by immunofluorescent analysis. (A) Propidum iodide; (B) p53; (C) merge of (A) and (B). (D) Western blotting of doxycycline-dependent p53 expression; β-actin was the internal control. WT, wild-type.

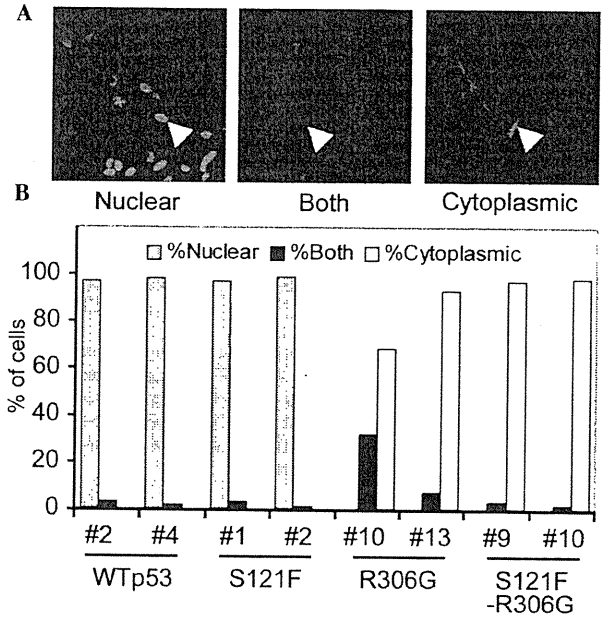

Figure 2. Quantitative analysis of the subcellular localization of wild-type p53 and S121F. (A) Subcellular localization of p53 was visualized as described in Fig. 1, and was classified as nuclear, cytoplasmic or both nuclear and cytoplasmic. (B) One hundred cells were analyzed and the percentage of each category is shown. WT, wild-type

category (wild-type, S121F, R306G, S121F-R306G and null p53) and estimated the viable cells at 24, 48 and 72 h after p53 induction by doxycycline (data not shown). The results at 48 h are shown in Fig. 3A. Although the cytoplasmic sequestration of wild-type p53 considerably disturbed the inhibitory effect against cell proliferation by wild-type p53, some inhibitory effects remained. The cytoplasmic sequestration of S121F did not disrupt the strong inhibitory effect on cell proliferation. These results indicate a cytoplasmic function of p53 on cell proliferation in both wild-type p53 and S121F.

Induction of apoptosis by cytoplasmically localized wild-type p53 and S121F. To evaluate the ability of wild-type p53 and the S121F mutant to induce apoptosis, each cell line was cultured and analyzed for a percentage of cell-cycle phase by fluorescence-activated cell sorting 24 h following the p53 induction by doxycycline (Fig. 3B and C). As shown in Fig. 3B, compared to the null p53 control, wild-type p53 clearly arrested cells at the G1 (49.9-59.4%) and G2 + M (12.3-32.1%) phases of the cell cycle and subsequently reduced the S-phase fraction (33.1-2.3%). The sub-G1 fraction (apoptosis fraction) was only slightly increased (4.7-6.2%) at 24 h, whereas at 48 h a substantial increase was observed (1.7-16.1%; data not shown). The cytoplasmic sequestration of p53 did not affect the cell cycle (G1, 60.5%; G2 + M, 31.6%), but slightly affected both the S phase (5.9%) and the sub-G1 phase (2%). S121F markedly increased the sub-G1 fraction (44.5%) without an increase in the G1 (33.1%) and G2 + M (8.3%) fractions, indicating strong apoptotic induction without cell cycle arrest. The cytoplasmic sequestration of S121F affected the sub-G1 (26.7%), G1 (41.2%) and G2 + M (19.6%) fractions only partially, indicating that a strong induction of apoptosis of S121F was retained despite the cytoplasmic sequestration. These results were consistent with the results of the cell proliferation analysis and again indicated a cytoplasmic function of p53 on both cell cycle arrest and apoptosis.

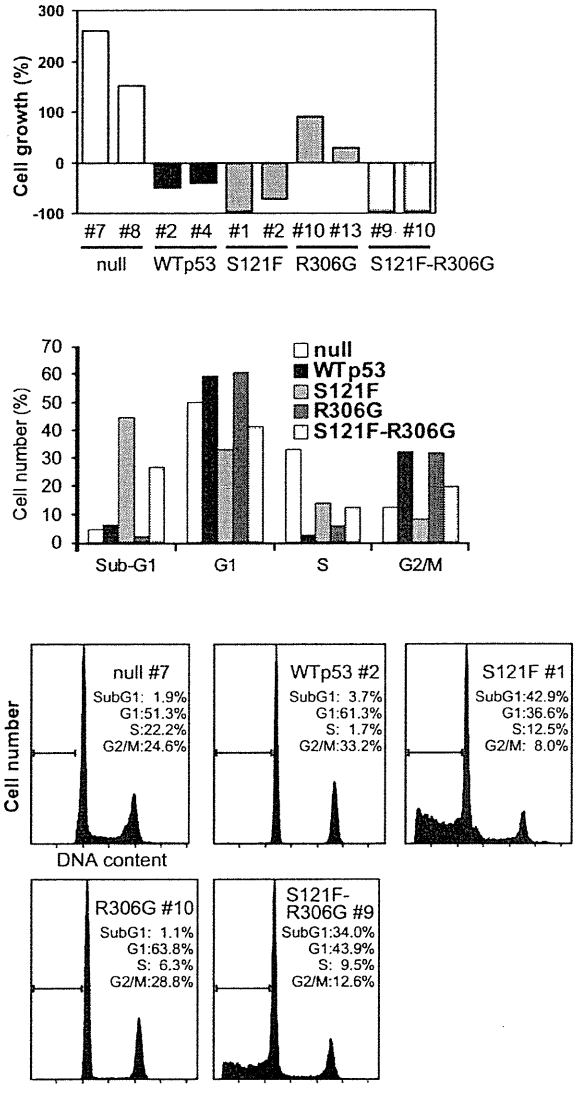

Figure 3. Inhibition of cell proliferation and induction of apoptosis by wild-type p53 and S121F. (A) Cell proliferation assays were performed at 24, 48 and 72 h after the addition of doxycycline. The average of triplicate data at 48 h is shown. (B) Cell cycle analysis by fluorescence-activated cell sorting. The average subfraction value of two independent cell lines at 24 h after the addition of doxycycline is shown. (C) Representative DNA histogram and subfractions at 24 h.

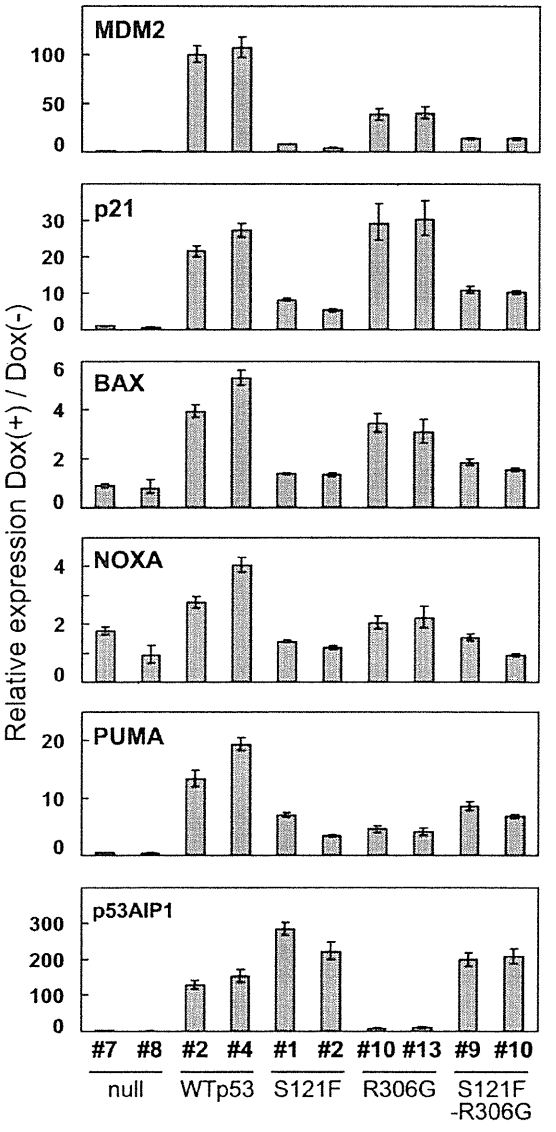

Figure 4. Transactivation of six p53 target genes by quantitative real-time PCR analysis. The expression level of each p53 target gene was collected by β-actin. Relative induced expression is shown as a ratio of the collected value of doxycycline presence against that of doxycycline absence. Two independent clones were analyzed, and the data are shown as a mean of four replicates with an error bar of standard deviation.

Transactivation of p53 target genes by cytoplasmically localized wild-type p53 and S121F. To examine the effect of cytoplasmic sequestration on transcriptional activation by wild-type p53 and S121F, transcripts of the p53-downstream genes, *MDM2*, *p21WAF1*, *BAX*, *NOXA*, *PUMA* and *p53AIP1*, were quantitated by real-time quantitative PCR analysis at 24 h after p53 induction (Fig. 4). Of the six genes, all except *p53AIP1* were less efficiently transactivated by S121F than by wild-type p53. The results showing a lower ability of S121F than wild-type p53 on transactivation were mostly consistent with our previous findings, with the exception of the result of *p53AIP1* (17), which is consistent with the previous hypothesis that S121F may cause a transactivation-independent apoptotic pathway. Notably, the cytoplasmic sequestration of wild-type p53 did not completely inactivate transactivation, but it reduced the level of transactivation in 5 of the 6 target genes (wiht the exception of *p21WAF1*). Of note, the cytoplasmic sequestration of S121F did not change the expression profile of the target genes. The ability of cytoplasmically sequestered S121F on transactivation was also confirmed when the expression level of each p53 target gene was collected by GAPDH (data not shown).

Discussion

The cytoplasmic sequestration of p53 did not completely inactivate p53 function, suggesting the cytoplasmic function of p53. This finding may be the reason that mutations on the

bipartite sequence in human tumors are extremely rare. In this context, Goldman *et al* showed that in a neuroblastoma cell line expressing cytoplasmically sequestered wild-type p53, p53 target genes (*p21WAF1* and *MDM2*) were up-regulated following cell irradiation (18). These results also suggest that wild-type p53 retains some functional activity when it is sequestered in the cytoplasm, although p53 homologues, such as p63 and p73, may have been involved in the result. By contrast, our experimental system was a p53-specific inducible system; therefore, involvement of p53 homologue activation is unlikely.

Our previous knowledge of p53-dependent apoptosis was that after genotoxic stress, activated p53 transactivated its downstream genes in a sequence-specific manner in the cell nucleus and induced apoptosis in cells through the direct or indirect induction of the downstream protein(s); however, a transactivation-independent mechanism for p53-dependent apoptosis has been reported by several laboratories (19,20). In addition, we previously indicated a lack of correlation between p53-dependent transactivation activity and the ability to induce apoptosis, and speculated that a transactivation-independent mechanism may exist (17). We excluded the nuclear function of p53, including the sequence-specific transactivation function, by introducing R306G, a mutation in the bipartite sequence at residues 305 and 306. A conditional expression system of cytoplasmically sequestered p53 was constructed and we found that cytoplasmically sequestered p53 retains its ability to arrest cell proliferation (wild-type p53) and induce apoptosis (S121F). These results strongly support a cytoplasmic apoptotic function of p53. Notably, however, cytoplasmically sequestered p53 transactivated downstream genes. Therefore, we did not clarify whether cytoplasmic p53-dependent apoptosis depends on either a direct or an indirect transactivation mechanism or is independent of transactivation.

Additional experiments are required to evaluate which mechanism is crucial for p53-dependent apoptosis and to clarify the mechanism underlying super p53 (S121F)-dependent apoptosis.

Acknowledgements

This study was supported by the Ministry of Education, Culture, Sports, Science and Technology (C. Ishioka and S. Kato), the Comprehensive Research and Education Center for Planning of Drug Development (CRECENDO) of Tohoku University 21st. Century COE Program (K. Yasuda and C. Ishioka), and the Gonryo Medical Foundation (C. Ishioka).

References

1. Hollstein M, Rice K, Greenblatt MS, *et al*: Database of p53 gene somatic mutations in human tumors and cell lines. Nucleic Acids Res 22: 3551-3555, 1994.
2. Soussi T: p53 alterations in human cancer: more questions than answers. Oncogene 26: 2145-2156, 2007.
3. Harris SL and Levine AJ: The p53 pathway: positive and negative feedback loops. Oncogene 24: 2899-2908, 2005.
4. Soussi T and Lozano G: p53 mutation heterogeneity in cancer. Biochem Biophys Res Commun 331: 834-842, 2005.
5. Moll UM, LaQuaglia M, Benard J and Riou G: Wild-type p53 protein undergoes cytoplasmic sequestration in undifferentiated neuroblastomas but not in differentiated tumors. Proc Natl Acad Sci USA 92: 4407-4411, 1995.
6. Moll UM, Riou G and Levine AJ: Two distinct mechanisms alter p53 in breast cancer: mutation and nuclear exclusion. Proc Natl Acad Sci USA 89: 7262-7266, 1992.
7. Nagpal J, Jamoona A, Gulati ND, *et al*: Revisiting the role of p53 in primary and secondary glioblastomas. Anticancer Res 26: 4633-4639, 2006.
8. Liang SH and Clarke MF: A bipartite nuclear localization signal is required for p53 nuclear import regulated by a carboxyl-terminal domain. J Biol Chem 274: 32699-32703, 1999.
9. Kim IS, Kim DH, Han SM, *et al*: Truncated form of importin alpha identified in breast cancer cell inhibits nuclear import of p53. J Biol Chem 275: 23139-23145, 2000.
10. Rodriguez-Lopez AM, Xenaki D, Eden TO, Hickman JA and Chresta CM: MDM2 mediated nuclear exclusion of p53 attenuates etoposide-induced apoptosis in neuroblastoma cells. Mol Pharmacol 59: 135-143, 2001.
11. Kaul SC, Deocaris CC and Wadhwa R: Three faces of mortalin: a housekeeper, guardian and killer. Exp Gerontol 42: 263-274, 2007.
12. Andrews P, He YJ and Xiong Y: Cytoplasmic localized ubiquitin ligase cullin 7 binds to p53 and promotes cell growth by antagonizing p53 function. Oncogene 25: 4534-4548, 2006.
13. Nikolaev AY, Li M, Puskas N, Qin J and Gu W: Parc: a cytoplasmic anchor for p53. Cell 112: 29-40, 2003.
14. Kato S, Han SY, Liu W, *et al*: Understanding the function-structure and function-mutation relationships of p53 tumor suppressor protein by high-resolution missense mutation analysis. Proc Natl Acad Sci USA 100: 8424-8429, 2003.
15. Freeman J, Schmidt S, Scharer E and Iggo R: Mutation of conserved domain II alters the sequence specificity of DNA binding by the p53 protein. EMBO J 13: 5393-5400, 1994.
16. Saller E, Tom E, Brunori M, *et al*: Increased apoptosis induction by 121F mutant p53. EMBO J 18: 4424-4437, 1999.
17. Kakudo Y, Shibata H, Otsuka K, Kato S and Ishioka C: Lack of correlation between p53-dependent transcriptional activity and the ability to induce apoptosis among 179 mutant p53s. Cancer Res 65: 2108-2114, 2005.
18. Goldman SC, Chen CY, Lansing TJ, Gilmer TM and Kastan MB: The p53 signal transduction pathway is intact in human neuroblastoma despite cytoplasmic localization. Am J Pathol 148: 1381-1385, 1996.
19. Chen X, Ko LJ, Jayaraman L and Prives C: p53 levels, functional domains, and DNA damage determine the extent of the apoptotic response of tumor cells. Genes Dev 10: 2438-2451, 1996.
20. Haupt Y, Rowan S, Shaulian E, Vousden KH and Oren M: Induction of apoptosis in HeLa cells by trans-activation-deficient p53. Genes Dev 9: 2170-2183, 1995.

Part 5

がん種別骨転移治療の実際をみる

6 原発不明がん骨転移に対する治療の実際をみる

Summary

原発不明がんは全悪性腫瘍の3～5%を占めており，原発不明がん全体における骨転移の頻度は30%程度と比較的上位を占める．原発不明がんで予後良好とされているサブグループの一つである，男性で造骨性転移のみ有しPSA値が上昇するケースにおいては，前立腺がんに準じた治療がおこなわれる．また，それ以外の骨転移を有する原発不明がんに対しては，一般的には全身的な治療としてプラチナ製剤とタキサン系薬剤の併用療法がおこなわれる．骨転移に対するマネジメントとしては，局所治療としての放射線療法やセメント注入術，骨関連事象の軽減を目的としたビスホスホネート（BP）製剤の投与などが考慮される．

骨転移と原発不明がん

骨転移はすべての担がん患者のうち約10%に認められ，おもな原発巣は肺がん，乳がん，前立腺がんが占める．しかし，骨転移に由来する痛みなどを初発症状とする患者に対して，CTなどの画像検査など注意深い全身検索をおこなっても原発巣の同定に至らないケースも存在する．その場合は原発不明がんとして取り扱われ治療をおこなう必要があるが，ここでは骨転移を伴う原発不明がんの臨床像や治療方法について述べる．

原発不明がんの臨床像

原発不明がんとは，臨床的に注意深い全身検索や経過観察をおこなっても原発巣が同定できず，組織学的に転移巣のみが判明している固形腫瘍を指す．原発不明がんの発生頻度は，近年の診断技術の向上により変化してきている可能性はあるが，おおむね全悪性腫瘍の3～5%と報告されている[1]．組織像の大半は腺がんあるいは未分化がんであり全体の80%程度を占める．臨床経過の過程で原発巣が判明するものは15～20%と報告されているが[2]，最終的に病理解剖に至っても2割程度は原発巣を同定することができない[3]．また原発巣が判明した場合，主要な原発性腺がんの分布とは異なっており，その原発巣は膵胆道系，肺であることが多い．また，転移がみられる臓器としては，リンパ節，肝，骨，肺の頻度が高い（表❶）[4]．

診断基準からわかるとおり原発不明がんは除外診断であるため，さまざまな腫瘍が混在した不均一な疾患群である．そのため同じ診断であっても

症例ごとにさまざまな臨床経過を辿る．とくに原発不明がんには，予後良好な臨床経過を辿るサブグループが存在することが知られている（表❷）[1]．これら患者群にはそれぞれ選択すべき治療法がある程度確立されているため，間違いなく診断して適切な治療を実践することが重要である[5]．

一方，表❷のサブグループ以外の原発不明がんには確立された治療方法はなく，一般的にプラチナ製剤とタキサン系薬剤の併用療法がおこなわれるが，予後は一般的に不良である．

骨転移を伴う原発不明がんの臨床像

前項に記載したように，原発不明がん全体における骨転移の頻度は高く，報告により異なるが全体の20～30％程度を占めていると思われる[4][6]．そのため，骨転移を契機に医療機関を受診するケースは比較的多いものと思われる．

医療機関受診時に原発巣が不明の骨転移患者に対して，CTなどの画像検査や骨生検などにより原発部位の診断がつくケースの場合，その原発巣の多くは肺，前立腺，乳腺，腎などである（表❸）[7]．しかし近年の画像検査の進歩や病理解剖などを経ても診断がつかないケースも20％程度みられるのが現状である．

一方，原発不明がんと診断された骨転移のパターンと，当初から原発巣が特定されている臓器がんからの骨転移パターンは異なっているという報告がある[8]．たとえば，肺がんと診断された患者の30～50％に骨転移が認められるのに対して，原発不明がんとして診断され後に肺が原発と診断されたケースでは4％でしか骨転移が認められなかったと報告されている．同様に，前立腺原発がもともと判明しているケースとくらべ，原発不明がんの診断の後に前立腺が原発と診断されたケースでは骨転移の頻度は3分の1程度しか認められない．しかし，膵がんの場合は逆に原発不明がんと診断されたケースのほうが骨転移の頻度は約4倍高いと報告されている．なぜ，本来の各臓器がんとは異なる転移パターンを呈するかについての生物学的基礎はよくわかっていない．

表❶　原発不明がん1,000症例の臓器別転移部位

転移部位	患者数	割合
リンパ節	418	42%
肝	331	33%
骨	**289**	**29%**
肺	263	26%
胸膜	112	11%
腹膜	90	9%
脳	64	6%
副腎	60	6%
皮膚	38	4%
骨髄	34	3%

（Hess KR *et al*, 1999[4]より改変引用）

骨転移を有する原発不明がんの予後について

これまでの報告では，予後良好なサブグループに含まれない原発不明がんの予後因子として，表

表❷　予後良好とされているサブグループ

① 女性で腋下リンパ節転移（腺がん）だけが認められるケース
② 女性で腹膜転移（腺がん）のみ有しCA125が上昇しているケース
③ 男性で造骨性転移のみ有しPSAの上昇しているケース
④ 頸部リンパ節転移（扁平上皮がん）のみ有するケース
⑤ 単径リンパ節転移のみ有するケース
⑥ 組織型が神経内分泌腫瘍であるケース
⑦ 比較的若年男性で正中線上に病変が分布し，β-HCG，AFPの上昇が認められる低・未分化がんのケース

（Pavlidis N *et al*, 2003[1]より改変引用）

表❸ 骨転移から診断された原発巣の内訳

報告者	年	前立腺	乳腺	腎臓	肺	甲状腺	その他	原発不明
Simon ら	1986	4	4	12	14	2	4	60
Nottebaert ら	1989	3	4	1	16	0	6	70
Rougraff ら	1993	0	3	10	62	3	12	10
Rougraff ら	1993	24	3	10	17	1	15	30
Alcalay ら	1995	28	6	7	13	1.5	5.5	39
Destombe ら	2000	17	13	5	24	0	20	21

各臓器の欄の数字は%を示す. (Destombe C *et al*, 2007[7]より改変引用)

表❹ 原発不明がんのおもな予後不良因子

報告者	患者数	予後不良因子
原発不明がん全般		
Abbruzzese ら	657 例	男性，腺がん，転移数，肝転移
Lortholary ら	311 例	男性，PS＞1，腺がん，転移数
Culine ら	150 例	PS＞1，LDH 高値
Sève ら	317 例	PS＞1，肝転移，合併症，リンパ球減少，LDH 高値，低アルブミン血症
低分化がんおよび腺がんの原発不明がん		
Hainsworth ら	220 例	35 歳以上，年間 10 箱以上の喫煙歴，後腹膜および末梢リンパ節転移以外の遠隔転移，LDH 高値
van der Gaast ら	77 例	PS＞0，ALP 高値
Lenzi ら	337 例	男性，64 歳以上，転移数（3 個以上）

(Culine S, 2009[9]より改変引用)

❹[9]のようなものがあげられている.

Hessら[4]は1,000例の原発不明がん患者を転移部位，転移臓器数，病理組織診断，年齢などに従って10クラスに分類し，それぞれのグループの予後について後方視的解析をおこない報告している．それによると，肝転移巣がない原発不明がん669例の生存期間の中央値は13ヵ月であり，そのなかでも骨転移症例(214例)については9ヵ月，骨転移が認められない症例（455例）では15ヵ月であったことを報告している．ただし，この報告のなかには予後良好なサブグループも含まれていると思われ，また治療情報についても言及されていない.

一方，Kodairaら[10]は，予後良好なサブグループを除いた（ただし女性で腹膜転移のみ有する腺がんのケースは含む）原発不明がん58例に対してカルボプラチンとパクリタキセルを用いた一次治療をおこなった成績を報告している．そのなかで彼らは多変量解析をおこなっており，骨転移とperformance status（PS）が予後と相関していることを報告しており，PS 0または1かつ骨転移がない群（good risk群19例）と，これらのどちらかを有する群（poor risk群39例）に分けて予後解析をおこなったところ，1年生存率はgood risk群で67.1％とpoor risk群で36.8％であることを報告している（p＝0.0003）．彼らの報告もまた後方視的解析で症例数は少ないものの，潜在性前立腺がん，乳がんケースは含まれていないこと，さらに58例すべてが，予後良好なサブグループを除いた原発不明がんに対して通常おこなわれるカルボプラチンとパクリタキセルの併用療法を用いた一次治療をおこなったうえでの成績であるこ